# Elastic Helmholtz resonators

A. N. Norris

Mechanical and Aerospace Engineering, Rutgers University, Piscataway, New Jersey 08855-0909

G. Wickhama)

The Ames Laboratory, Institute for Physical Research and Technology, Iowa State University, Ames, Iowa 50011

(Received 15 July 1992; revised 2 October 1992; accepted 2 October 1992)

The influence of wall elasticity on the response of a Helmholtz resonator is examined by analyzing the canonical case of a thin elastic spherical shell with a circular aperture subject to plane wave excitation. By neglecting the thickness of the wall and representing the elasticity via a "thin shell" theory the problem is reduced to one of solving an integral equation over the aperture for the polarization velocity, which is related to, but distinct from, the radial particle velocity of the fluid. The integral equation can be solved by asymptotic methods for small apertures, yielding closed-form expressions for the major resonator parameters. In general, wall compliance reduces the resonance frequency in comparison with an identically shaped rigid cavity. The Q value of the resonance is increased and the scattering strength of the cavity at resonance is enhanced by wall compliance. The asymptotic results are supported and supplemented by numerical calculations for thin steel shells in water.

PACS numbers: 43.20.Ks, 43.20.Rz, 43.30.Ky, 43.55.Ev

# INTRODUCTION

The Helmholtz resonator is characterized by a volume of compressible fluid connected to the exterior via a small opening. The inertia of the fluid entrained in the neighborhood of the opening conspires with the compressibility of the enclosed volume to produce a resonance frequency whose acoustic wavelength may be considerably longer than the maximum dimension of the vessel. This long wavelength or low-frequency nature of the resonance makes the phenomenon quite distinctive, as it tends to accentuate this mode as compared with others at higher frequencies. In most circumstances it is perfectly reasonable to consider the vessel enclosing the resonating fluid as rigid, which is the basis for the successful explanations of Helmholtz and Rayleigh for the resonance phenomenon. The rigid cavity idealization is certainly adequate in air but may need to be reconsidered if the acoustic fluid is water and the cavity is a thin shell. In this paper we consider the canonical geometry of a spherical elastic resonator with a circular aperture excited by an incident acoustic wave.

The approach taken here is to model the wall of the cavity as a *thin shell* of negligible thickness across which the normal velocity is continuous but nonzero. The explicit form of the thin shell theory used is of secondary importance, although a specific theory is adopted for numerical computations. The concept of a *polarization* velocity is used to reduce the scattering problem to one of solving an integral equation for the unknown polarization velocity on the aperture, similar to the problem for the rigid resonator. In fact, the rigid limit is simply obtained from the general theory

developed here. The problem is formulated in Sec. I within the context of an arbitrarily shaped cavity. Several transformations are employed in Sec. II to reduce the singular integral equation for a spherical cavity with a circular aperture to a relatively well-behaved set of linear equations. In Sec. III we develop some asymptotic approximations, valid in the small aperture limit. These results imply simple relations for the effective mass and capacitance of the elastic resonator, and comparisons are made with both the rigid case and to some related published findings for an elastic Helmholtz resonator. Numerical computations for rigid and elastic resonators are presented in Sec. IV.

Before commencing we note that detailed treatments of the corresponding rigid spherical resonator have been given by many authors, among whom we mention Rayleigh<sup>3</sup> and Levine, who have obtained successively better asymptotic approximations to the resonance frequency in the small aperture limit. Related results for the elastic resonator will be presented in Sec. III. The elasticity of the cavity can be significant if the fluid loading is large, which could occur in underwater applications. A paper by Henriquez and Young<sup>5</sup> discussed practical issues related to the design and use of low-frequency underwater Helmholtz resonators. In the present paper the mechanism that excites the resonator is a simple plane wave. For more complicated excitations associated with vortices we refer to Howe.6 Also, no internal dissipation is considered here, our objective being to describe the contribution of the wall elasticity. The only damping is from radiation loss. However, it is well known<sup>7.6</sup> that dissipation due to viscosity and heat conduction greatly exceeds the radiation loss in air. These mechanisms must certainly be taken into account for a complete description of the resonator. Finally, we note that the present treatment of the Helm-

a) Permanent address: The Department of Mathematics, University of Manchester, Manchester M13 9PL, UK.

holtz resonator includes the possibility of singular but integrable velocity fields at the aperture edge. As noted by Ingard, <sup>7</sup> a thorough analysis of the problem should include nonlinear effects and realistic treatments of sharp corners.

#### I. THE GENERAL THEORY

We consider time harmonic motion of radial frequency  $\omega$ . The term Re[ $\cdots e^{-i\omega t}$ ] will be understood but omitted everywhere. Our main object is to analyze the specific case of a spherical resonator of radius a with a circular mouth or aperture of semi-angle  $\alpha$ , see Fig. 1. Spherical polar coordinates r and  $\theta$  are used, where  $\theta = 0$  is the center of the mouth, and no assumptions are made at this stage about the size of the opening. The related problem of a cylindrical resonator of infinite length with an opening in the form of an arc may be treated by similar methods. The details are in Appendix C. However, it is both convenient and instructive to first formulate the scattering problem for a thin elastic cavity of arbitrary shape with a general aperture, which we will do in this section, proceeding to the specific case of interest in the next section. The general method is based upon the use of a polarization velocity across the aperture, which allows us to reduce the issue to an integral equation over the same region. Applications of this approach to other scattering problems in acoustics and elasticity are discussed by Wickham.8

Let p denote the acoustic pressure in the fluid and w the outward normal velocity on the shell. The pressure satisfies the Helmholtz equation in the fluid, which is assumed to be inviscid and occupying both the interior (r < a) and the exterior (r > a) of the resonator. Thus, at all points excepting sources, the total pressure satisfies

$$\nabla^2 p + k^2 p = 0, \text{ in the fluid,} \tag{1}$$

where  $k = \omega/c$  and c is the sound speed. The jump in pressure across the shell is defined as

$$[p](\theta) = p(a - 0, \theta) - p(a + 0, \theta).$$
 (2)

The actual pressure jump across a shell of thickness h is  $[p(a-h/2,\theta)-p(a+h/2,\theta)]$ . However, if the acoustic wavelength is much greater than h then it is justifiable to take the limit of  $h \rightarrow 0$ . The present analysis could be developed with the jump for finite values of the shell thickness. However, for simplicity we neglect this effect as a higher order contribution to the resonance.

The equations on the shell are

$$w = L^{-1}[p],$$

$$0 = \left[\frac{\partial p}{\partial r}\right],$$

$$w = (i\rho\omega)^{-1}\frac{\partial p}{\partial r},$$

$$r = a, \text{ on the shell.}$$
(3)

The first condition defines the equation of motion of the shell. The quantity L denotes an operator on w, which will generally include supplementary equations for the insurface compounds of the velocity of the shell. Specific examples of L are presented in Appendix A, but for the moment we will keep it general. The inverse operator  $L^{-1}$  is used specifically to emphasize that there are additional *edge conditions* that must be satisfied at the edges of the shell, which defines the

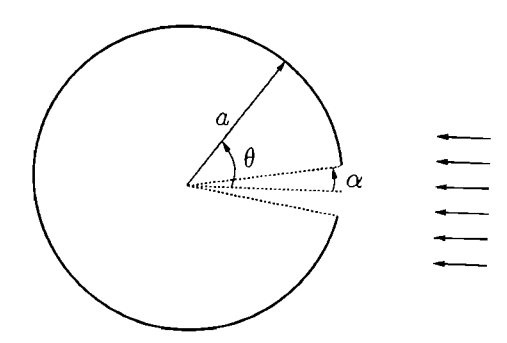


FIG. 1. The geometry of the spherical shell resonator of radius a with aperture semiangle a. The numerical results in Sec. V consider the incident plane wave shown.

mouth. The edge conditions are implicitly accounted for in  $L^{-1}$ . In the present case, where the fluid is assumed to be inviscid, the bending moment and shear must vanish at the edges. The inverse operator  $L^{-1}$  is the Green's operator for the fluid-loaded finite shell, and could be represented as a convolution integral operator with the kernel being the Green's function. If L were a scalar then it could be identified as the local shell impedance. The second condition in (3) states that the radial velocity in the fluid is continuous across the shell. The third condition stipulates that the fluid and shell radial velocities are identical, where  $\rho$  is the fluid mass density per unit volume. Across the mouth the pressure and radial velocity must be continuous, implying the complementary conditions

We decompose the total solution into two parts:

$$p = p^{(0)} + p^{(1)}, (5a)$$

$$w = w^{(0)} + w^{(1)}. (5b)$$

Here,  $p^{(0)}$  and  $w^{(0)}$  contain the incident fields and the response from the complete shell, i.e., as if the mouth were not there. The solution for the full shell satisfies

$$w^{(0)} = L^{-1}[p^{(0)}],$$

$$\left[\frac{\partial p^{(0)}}{\partial r}\right] = 0,$$

$$w^{(0)}(\theta) = (i\rho\omega)^{-1} \frac{\partial p^{(0)}}{\partial r},$$

$$r = a, \text{ all } \theta.$$
(6)

The effects of the mouth are described by the additional fields  $p^{(1)}$  and  $w^{(1)}$ . The full-shell response is the driving force for the additional pressure and shell vibration, which solve, from Eqs. (3)-(6).

$$w^{(1)} - L^{-1}[p^{(1)}] = 0$$
 on the shell,  
 $[p^{(1)}] = -[p^{(0)}]$ , on the mouth, (7)

and

$$\left[\frac{\partial p^{(1)}}{\partial r}\right] = 0,$$

$$w^{(1)}(\theta) = (i\rho\omega)^{-1} \frac{\partial p^{(1)}}{\partial r},$$

$$r = a, \text{ all } \theta.$$
(8)

We now introduce the *velocity polarization*,  $W(\theta)$ , defined as

$$W(\theta) = w - L^{-1}[p]$$
  
=  $w^{(1)} - L^{-1}[p^{(1)}].$  (9)

It is clear from  $(7)_1$  that the polarization vanishes for all values of  $\theta$  except on the mouth, where from  $(7)_2$  we have

$$LW(\theta) - Lw^{(1)} = [p^{(0)}], \text{ on the mouth.}$$
 (10)

Equation (10) turns out to be the crucial relation which must be solved for  $W(\theta)$  in order to calculate the response of the shell cavity. First, however, we must use (9) to eliminate  $Lw^{(1)}$  in favor of  $W(\theta)$ , which requires using the acoustic Green's function associated with the particular geometry. However, as we will see, there is no need to explicitly involve the Green's function for the spherical geometry considered here. We note that the classical case of a rigid enclosure may be considered by taking L to be a scalar and then letting  $L \to \infty$ . In general, the total radial velocity may be written

$$w(\theta) = W(\theta) + L^{-1}[p]. \tag{11}$$

In the rigid limit W is just the radial velocity on the mouth, but in general the polarization does not have this simple interpretation.

#### II. APPLICATION TO THE SPHERICAL RESONATOR

# A. The full shell solution

Before solving the integral equation for the shell with the mouth present, we present the solution to (6) for the full shell subject to an incident wave of the form

$$p^{\text{inc}} = \sum_{n=0}^{\infty} C_n j_n(kr) P_n(\cos \theta), \tag{12}$$

where  $j_n$  are spherical Bessel functions of order n and  $P_n$  are the Legendre polynomials. The constants  $C_n$  in (12) define the type of incident wave. For instance,  $C_n = (2n+1)(-i)^n$  if the incident wave is the plane wave  $p^{\text{inc}} = e^{-ikr\cos\theta}$  propagating directly into the mouth, see Fig. 1. It is easily shown by standard separation of variables that

$$p^{(0)} = p^{\text{inc}} - \sum_{n=0}^{\infty} C_n \frac{Z_n^r}{Z_n^r + Z_n^r}$$

$$\times P_n(\cos \theta) \begin{cases} j_n(kr), & \text{for } r \leq a, \\ \frac{j'_n(ka)}{h'_n(ka)} h_n(kr), & \text{for } r \geq a. \end{cases}$$
(13)

Here,  $h_n$  are spherical Hankel functions of the first kind of order n, and the scalars  $Z_n^f$  and  $Z_n^x$  are impedances associated with the fluid and shell,

$$Z_{n}^{f} = \frac{\rho c}{(ka)^{2} j'_{n}(ka) h'_{n}(ka)}.$$
 (14)

The shell impedances are the eigenvalues of the shell operator L for normal velocity  $w = P_n(\cos \theta)$ , i.e., they are defined by

$$LP_n(\cos\theta) = Z_n P_n(\cos\theta), \tag{15}$$

for each n = 0,1,2,.... The existence of Legendre polynomials as pure modes follows from the symmetry of the full

sphere, although the precise values of  $Z_n^s$  depend upon the particular thin-shell theory used. A specific example will be considered later (see Appendix A). Finally, we note that the  $p^{(0)}$  solution is quite distinct from the solution for the spherical shell which is empty, i.e., the pressure vanishes on the interior surface. In that case the solution for r < a is irrelevant, but the solution in the exterior can be represented in the same manner, but with the replacement

$$\frac{Z_n^s}{Z_n^s + Z_n^f} \rightarrow \frac{Z_n^s + i\rho c \left[ j_n(ka) / j_n'(ka) \right]}{Z_n^s + i\rho c \left[ h_n(ka) / h_n'(ka) \right]}.$$
 (16)

It is important to remember this difference, since most numerical results in the literature are for empty shells, or for shells loaded by water on the outside with air inside, the which are almost identical in their response to the empty shell.

# B. The kernel

Let the mouth be centered at the north pole,  $\theta = 0$  in spherical polar coordinates, with extent  $0 \le \theta < \alpha$ . We assume, for simplicity, that the total response possesses azimuthal symmetry about the direction  $\theta = 0$ . Then the radial velocity due to the presence of the mouth may be expanded as

$$w^{(1)}(\theta) = \sum_{n=0}^{\infty} A_n P_n(\cos \theta), \tag{17}$$

where  $A_n$  are to be determined. The pressure in the fluid follows from (8) as

$$p^{(1)} = i\rho\omega \sum_{n=0}^{\infty} A_n P_n(\cos\theta) \begin{cases} \frac{h_n(kr)}{kh'_n(ka)}, & r > a, \\ \frac{j_n(kr)}{kj'_n(ka)}, & r < a. \end{cases}$$
(18)

It now follows from (2), (15), (17), (18) and the Wronskian relation for spherical Bessel functions, 12 that

$$w^{(1)} - L^{-1}[p^{(1)}] = \sum_{n=0}^{\infty} \frac{Z_n^s + Z_n^f}{Z_n^s} A_n P_n(\cos \theta).$$
(19)

Substituting from (9) for the left member in (19) and then taking inner products with  $P_n(\cos \theta)$ , using the fact that  $W(\theta) = 0$  for  $\theta > \alpha$ , gives<sup>12</sup>

$$A_{n} = \left(n + \frac{1}{2}\right) \frac{Z_{n}^{s}}{Z_{n}^{f} + Z_{n}^{s}} \int_{0}^{\alpha} W(\theta')$$

$$\times P_{n}(\cos \theta') \sin \theta' d\theta. \tag{20}$$

It follows from (15), (17), and (20) that

$$Lw^{(1)} = \sum_{n=0}^{\infty} \left( n + \frac{1}{2} \right) \frac{\left( Z_n^s \right)^2}{Z_n^f + Z_n^s} P_n(\cos \theta)$$

$$\times \int_0^{\alpha} W(\theta') P_n(\cos \theta') \sin \theta' \, d\theta'. \tag{21}$$

We note the identity

$$LW(\theta) = \sum_{n=0}^{\infty} \left( n + \frac{1}{2} \right) Z_n^s P_n(\cos \theta)$$

$$\times \int_0^{\alpha} W(\theta') P_n(\cos \theta') \sin \theta' d\theta', \qquad (22)$$

which follows by expanding W as a Legendre series and then using (15). Subtracting (21) from (22) and using (10) we finally deduce the desired integral equation for  $W(\theta)$ ,

$$\int_0^\alpha W(\theta')K(\theta,\theta')\sin\theta'\,d\theta' = [p^{(0)}](\theta), \quad 0 \le \theta < \alpha.$$
(23)

The kernel  $K(\theta, \theta') = K(\theta', \theta)$  is

$$K(\theta, \theta') = \sum_{n=0}^{\infty} K_n P_n(\cos \theta) P_n(\cos \theta'), \tag{24}$$

where

$$K_n = \left(n + \frac{1}{2}\right) \frac{Z_n^f Z_n^s}{Z_n^f + Z_n^s}.$$
 (25)

Equation (23) is a Fredholm integral equation of the first kind with a symmetric kernel. Note that the effective impedance in  $K_n$  is the result of the enclosed fluid and shell acting in series, as one might expect. The integral equation for the rigid cavity is of exactly the same form with  $W(\theta) = w(\theta)$ , the total velocity on the mouth. The kernel is the same with the effective impedance given by the limit of  $Z_n^s \to \infty$ , i.e.,

$$K_n = (n + \frac{1}{2})Z_n^f, \quad \text{rigid.} \tag{26}$$

# C. An infinite set of equations

We wish to solve the integral equation (23) for the polarization  $W(\theta)$  on the mouth  $0 \le \theta \le \alpha$ . The polarization, although it vanishes for  $\theta > \alpha$ , may behave in a singular, but integrable, manner as  $\theta \to \alpha$ . Examination of the shell equations in Appendix A shows that the singularity for W is the same as that for a rigid enclosure:  $W \sim (\alpha - \theta)^{-1/2}$ ,  $\theta \uparrow \alpha$ . The singular part of  $W(\theta)$  can be removed in the following manner. Expand the forcing in Eq. (23) in terms of Legendre polynomials

$$[p^{(0)}](\theta) = \sum_{n=0}^{\infty} [p_n^{(0)}] P_n(\cos \theta), \tag{27}$$

where the coefficients  $[p_n^{(0)}]$  for the incident wave of Eq. (12) are

$$[p_n^{(0)}] = \frac{Z_n^s}{Z_n^f + Z_n^s} [p_n^{(rig)}], \qquad (28)$$

and  $[p_n^{(rig)}]$  are the coefficients of the pressure jump for the rigid sphere,

$$[p_n^{(rig)}] = \frac{-iC_n}{(ka)^2 h'_n(ka)}.$$
 (29)

Now using (24) and the Mehler–Dirichlet integral representation for the Legendre polynomials<sup>13</sup>

$$P_n(\cos\theta) = \frac{\sqrt{2}}{\pi} \int_0^\theta \frac{\cos(n + \frac{1}{2})u}{\sqrt{\cos u - \cos \theta}} du, \tag{30}$$

the integral equation (23) may be written as

$$0 = \frac{\sqrt{2}}{\pi} \int_0^\theta \frac{du}{\sqrt{\cos u - \cos \theta}} \left\{ \int_0^\alpha \sin \theta' W(\theta') \right\}$$

$$\times \left[ \sum_{n=0}^\infty K_n P_n(\cos \theta') \cos \left( n + \frac{1}{2} \right) u \right] d\theta'$$

$$- \sum_{n=0}^\infty \left[ p_n^{(0)} \right] \cos \left( n + \frac{1}{2} \right) u \right\}. \tag{31}$$

Because this holds for all  $\theta$ ,  $0 \le \theta \le \alpha$ , it follows that

$$\int_{0}^{\alpha} \sin \theta' W(\theta') \frac{\sqrt{2}}{\pi} \int_{0}^{\theta'} \frac{1}{\sqrt{\cos v - \cos \theta'}} \times \left[ \sum_{n=0}^{\infty} K_{n} \cos \left( n + \frac{1}{2} \right) u \cos \left( n + \frac{1}{2} \right) v \right] dv d\theta'$$

$$= \sum_{n=0}^{\infty} \left[ p_{n}^{(0)} \right] \cos \left( n + \frac{1}{2} \right) u, \quad 0 \le u < \alpha.$$
 (32)

Note that (30) has been used again here. Now interchange the order of integration in (32), to give

$$\int_0^\alpha H(u,v)q(v)dv$$

$$= \sum_{n=0}^\infty \left[p_n^{(0)}\right] \cos\left(n + \frac{1}{2}\right)u, \quad 0 \le u < \alpha,$$
(33)

with

$$H(u,v) = \sum_{n=0}^{\infty} K_n \cos\left(n + \frac{1}{2}\right) u \cos\left(n + \frac{1}{2}\right) v, \quad (34)$$

and

$$q(v) = \frac{\sqrt{2}}{\pi} \int_{v}^{a} \frac{W(\theta)\sin\theta}{\sqrt{\cos v - \cos\theta}} d\theta.$$
 (35)

Equation (35) is an Abel integral equation for the determination of W. Its solution is

$$W(\theta) = \frac{-1}{\sqrt{2}\sin\theta} \frac{d}{d\theta} \int_{\theta}^{a} \frac{q(u)\sin u \, du}{\sqrt{\cos\theta - \cos u}} \,. \tag{36}$$

This can be further simplified as

$$W(\theta) = \frac{1}{\sqrt{2}} \frac{q(\theta)}{\sqrt{\cos \theta - \cos \alpha}} - \frac{1}{\sqrt{2}} \int_{\theta}^{\alpha} \frac{q'(u)du}{\sqrt{\cos \theta - \cos u}}.$$
 (37)

This form clearly shows the singular behavior of W at the mouth edge, and implies that q is smoothly behaved and bounded function over the entire month, including positions arbitrarily close to the edges.

The transformed integral equation (33) is therefore more desirable than the original integral equation (23) for the polarization. We now look for a solution to q in terms of a complete orthogonal set of functions on  $[0,\alpha]$ . We assume

$$q(v) = \sum_{n=0}^{\infty} q_n \cos n\pi \frac{v}{\alpha}.$$
 (38)

Substitute this expansion into the integral equation (33), then multiply by  $\cos m\pi u/\alpha$  and integrate over u. This gives the algebraic system of equations

$$\sum_{n=0}^{\infty} q_n M_{nm} = \sum_{n=0}^{\infty} \left[ p_n^{(0)} \right] p_{nm}, \tag{39}$$

where

$$M_{nm} = \sum_{l=0}^{\infty} K_l p_{ln} p_{lm}, \qquad (40)$$

and

$$p_{ln} = \int_0^\alpha \cos\left(l + \frac{1}{2}\right) v \cos n\pi \frac{v}{\alpha} dv$$

$$= (-1)^n \frac{(l+\frac{1}{2})\sin(l+\frac{1}{2})\alpha}{(l+\frac{1}{2})^2 - (n\pi/\alpha)^2}.$$
 (41)

Notice that the matrix M is symmetric.

In summary, the main problem is to solve the system of equations (40), which amounts to inverting a truncated version of the symmetric matrix M. We will see below that this becomes relatively simple in the limit of low frequency and small  $\alpha$ , for which we need only consider the single term  $M_{00}$ . The singular behavior of the velocity polarization at the mouth edge has been removed by the introduction of the function  $q(\theta)$ , which is defined only on the mouth. Once  $q(\theta)$ , or equivalently its moments  $q_n$ , has been obtained, the scattered field due to the mouth follows from (18) and (20). The integral in (20) may be simplified, using (30), (35), (38), and (41), as

$$\int_0^\alpha P_n(\cos\theta) W(\theta) \sin\theta \, d\theta = \sum_{m=0}^\infty P_{nm} q_m. \tag{42}$$

The additional radiated pressure caused by the mouth may then be written, from (18), (20), (25), and (42), as

$$p^{(1)} = i(ka)^2 \sum_{n=0}^{\infty} \left( K_n j_n'(ka) \sum_{m=0}^{\infty} p_{nm} q_m \right)$$
$$\times h_n(kr) P_n(\cos \theta). \tag{43}$$

The radial displacement, both on the mouth and the shell, follows from (18), (20), and (42). Finally, we note that the polarization, which is nonzero only on the mouth and singular at the edges, may be expressed as

$$W(\theta) = \sum_{n=0}^{\infty} q_n W_n(\theta), \tag{44}$$

where the functions  $W_n(\theta)$  are given by (37) with  $q(\theta) = \cos n\pi\theta/\alpha$ . The integral in (37) may be reduced to an infinite sum by the use of the identity,<sup>13</sup>

$$\frac{1}{\sqrt{\cos \theta - \cos u}}$$

$$= \sqrt{2} \sum_{m=0}^{\infty} P_m(\cos \theta) \sin\left(m + \frac{1}{2}\right) u, \quad u > \theta. \tag{45}$$

We find

$$W_{n}(\theta) = \frac{1}{\sqrt{2}} \frac{\cos n\pi\theta/\alpha}{\sqrt{\cos \theta - \cos \alpha}} + \frac{n\pi}{2\alpha} \sum_{m=0}^{\infty} P_{m}(\cos \theta) \times \left(\frac{2n\pi}{\alpha} \frac{\sin(m + \frac{1}{2})\alpha}{\left[(m + \frac{1}{2})^{2} - (n\pi/\alpha)^{2}\right]} + \frac{\sin(m + \frac{1}{2} + n\pi/\alpha)\theta}{m + \frac{1}{2} + n\pi/\alpha} - \frac{\sin(m + \frac{1}{2} - n\pi/\alpha)\theta}{m + \frac{1}{2} - n\pi/\alpha}\right).$$

$$(46)$$

These functions clearly display the singular behavior at the edges and thus they provide a suitable basis set for obtaining a uniformly convergent series for the polarization. It is difficult to imagine how one might have predicted the form of the  $W_n(\theta)$  prior to performing the analysis in this section. On the other hand, if we were to be content with a nonuniformly convergent representation we could follow the method used by Vinogradov et al.14 For the special case of a rigid shell the latter authors proceed from the slightly different perspective of dual series equations. Those are solved by noting that, in the static limit  $ka \rightarrow 0$ , the integral operator in (23) has an explicit inverse. It then follows that for all ka > 0, their dual series equation or, equivalently, (23) may be recast as a certain Fredholm second-kind system of algebraic equations whose "kernel matrix" appears as a perturbation about the static solution. In deriving (39) we have set out to explicitly obtain the singular behavior of  $W(\theta)$  and we conclude that our algebraic system is simply the appropriate rearrangement of that given in Ref. 14.

#### III. ASYMPTOTIC ANALYSIS OF THE RESONANCE

We now analyze the Helmholtz resonance in detail, taking advantage of the small parameters in the problem. By assumption, the resonance is a low-frequency phenomenon, so we assume that  $ka \le 1$ . The corresponding asymptotic behavior of the acoustic impedances of Eq. (14) are as follows:

$$Z_0^f = i \frac{\rho c}{ka} 3 \left( 1 - \frac{2}{5} (ka)^2 - \frac{i}{3} (ka)^3 + \cdots \right), \quad (47a)$$

$$Z_1^f = -i\rho cka \frac{3}{2} \left( 1 + \frac{3}{10} (ka)^2 + \frac{i}{6} (ka)^3 + \cdots \right), \tag{47b}$$

$$Z_n^f = -i\rho cka \frac{(2n+1)}{n(n+1)} + O((ka)^3), \quad n \geqslant 2.$$
 (47c)

Note that to leading order  $Z_0^f$  is a stiffness, whereas all the other  $Z_n^f$ ,  $n \ge 1$ , are mass-like. The low-frequency behavior of the shell impedances follow from Appendix A as

$$Z_0^s = i \frac{\rho c}{ka} \left( \frac{2}{\eta} (1 + \nu) \frac{c_p^2}{c^2} - \frac{1}{\eta} (ka)^2 + \cdots \right),$$
 (48a)

$$Z_1^s = -i\rho cka\left(\frac{3}{\eta} + \frac{2}{(1+\nu)\eta}\frac{c_p^2}{c^2}(ka)^2 + \cdots\right),$$
(48)

$$Z_n^s = i \frac{\rho c}{ka} \frac{c_\rho^2}{\eta c^2} \left[ (1 - v^2) \left( \frac{\lambda_n - 2}{\lambda_n - 1 + v} \right) + \beta^2 \lambda_n^2 \right] + O((ka)^2), \quad n \ge 2.$$
 (48c)

Note that  $Z_1^s$  is purely mass-like, all the others are pure stiffnesses. In the following we will not use these specific forms of the shell impedances. The only thing required is that the shell, whatever it may be, has the same low-frequency behavior for its impedances, in that all of them are stiffness-like except for the n=1 impedance, which is mass-like. Also, we are not including any loss terms in the shell in this analysis, so that the shell impedances are purely imaginary with zero real parts.

We now make the further assumptions that (1) the mouth opening is small,  $\alpha \ll 1$ , and (2) the resonance is governed by the low-frequency behavior of the single element  $M_{\infty}$ . This is equivalent to saying that the polarization near resonance is dominated by the first term in its expansion. The accuracy of this assumption is borne out by the numerical results. The exact form of  $M_{\infty}$  follows from (25), (40), and (41) as

$$M_{\infty} = \sum_{n=0}^{\infty} \frac{Z_n^f Z_n^s}{Z_n^f + Z_n^s} \frac{\sin^2(n + \frac{1}{2})\alpha}{n + \frac{1}{2}}.$$
 (49)

Taking into account the asymptotic form of the impedances, and anticipating the final dependence upon  $\alpha$ , this may be approximated as

$$M_{00} = Z_{0K}^{f} \left[ 2 \sin^{2} \frac{\alpha}{2} R_{0} \left( 1 - \frac{2}{5} \overline{R}_{0} (ka)^{2} - \frac{i}{3} R_{0} (ka)^{3} \right) - \left( \frac{2}{3} D(\alpha) - \frac{1}{3} R_{1} \sin^{2} \frac{3}{2} \alpha \right) (ka)^{2} \right],$$
 (50)

where

$$R_0 = \frac{Z_{0K}^s}{Z_{0K}^f + Z_{0K}^s}, \quad R_1 = \frac{Z_{1M}^f}{Z_{1M}^s + Z_{1M}^f}. \tag{51}$$

Here,  $Z_{0K}^f$  and  $Z_{0K}^s$  denote the leading order stiffness contributions to  $Z_0^f$  and  $Z_0^s$ , while  $Z_{1M}^f$  and  $Z_{1M}^s$  are the leading order mass-like parts of  $Z_1^f$  and  $Z_1^s$ . The number  $\overline{R}_0$  depends upon the next term in  $Z_0^s$ , and for the thin shell theory described by (48a) it is

$$\overline{R}_0 = R_0 + (1 - R_0) \frac{4}{5(1 + \nu)} \frac{c^2}{c_a^2}.$$
 (52)

The real-valued function  $D(\alpha)$  in (50) is

$$D(\alpha) = \sum_{n=1}^{\infty} \frac{\sin^2(n + \frac{1}{2})\alpha}{n(n+1)}$$
$$= \left(\frac{\pi}{2} - \alpha\right) \sin \alpha + \sin^2 \frac{\alpha}{2}.$$
 (53)

Details on the evaluation of the infinite sum may be found in Appendix B. The form of  $M_{00}$  in (50) is motivated by the desire to find both the real resonance frequency and the width of the resonance. Note that no explicit approximations have yet been made using the fact that  $\alpha$  is also small. We note that for the thin shell model of Appendix A,

$$R_{0} = \left(1 + \frac{a}{h} \frac{3\rho c^{2}}{2(1+\nu)\rho_{s}c_{p}^{2}}\right)^{-1},$$

$$R_{1} = \left(1 + \frac{a}{h} \frac{\rho}{2a}\right)^{-1},$$
(54)

where the parameters are defined in Appendix A. Hence, both  $R_0$  and  $R_1$  tend to zero for very thin shells  $(h/a \rightarrow 0)$  and to unity for very stiff and dense shells  $(\rho c^2/\rho_s c_p^2 \rightarrow 0, \rho/\rho_s \rightarrow 0)$ .

Setting the real part of  $M_{\infty}$  to zero we see from (50) that the resonance frequency occurs at  $k \approx k_0$ , where

$$k_0 = \sqrt{R_0 S / V \delta} \ . \tag{55}$$

Here we have written the resonance frequency in classical form, with  $S = 2\pi a^2 (1 - \cos \alpha)$  the spherical area of the mouth,  $V = 4\pi a^3/3$  the cavity volume, and  $\delta$  is the "end correction" for the aperture, which follows from (50) as

$$\delta = a \left( D(\alpha) + \frac{6}{5} R_0 \overline{R}_0 \sin^2 \frac{\alpha}{2} - \frac{1}{2} R_1 \sin^2 \frac{3}{2} \alpha \right).$$
 (56)

Thus, the effect of the elastic stiffness is to increase the end correction, while the mass contributions decreases it. However, it should be borne in mind that both effects are of second order in  $\alpha$  since  $D(\alpha) = \alpha \pi/2 + O(\alpha^2)$  for small apertures. The Q value of the resonance, defined in Eq. (60) below, also follows from (50) as

$$Q = 4\pi/R_0 k_0^3 V. {57}$$

These approximations have been deduced under the assumption that ka is small at resonance, which is true only if  $\alpha$  is also small. We can now take the limiting forms for these expressions for  $\alpha \ll 1$ , giving

$$k_0 a = \left(\frac{3\alpha}{2\pi}\right)^{1/2} R_0^{1/2} \times \left[1 + \frac{3\alpha}{4\pi} \left(1 - \frac{2}{5} R_0 \overline{R}_0 + \frac{3}{2} R_1\right) + \cdots\right], \quad (58a)$$

$$Q = 3\left(\frac{2\pi}{3\alpha}\right)^{3/2} R_0^{-5/2} + \cdots$$
 (58b)

We have retained enough terms so that the expansion for the resonance frequency agrees with the expansion found by Rayleigh<sup>3</sup> for the rigid cavity, which follows by setting  $R_0 = \overline{R}_0 = 1$  and  $R_1 = 0$ , yielding

$$k_0 a = \sqrt{\frac{3\alpha}{2\pi}} \left( 1 + \frac{9\alpha}{20\pi} + \cdots \right). \tag{59}$$

The subsequent term, of order  $\alpha^2$ , in the expansion for the rigid cavity has been derived by Levine.<sup>4</sup>

Thus, to leading order the elasticity of the cavity decreases the resonance frequency and increases the Q value of the resonance. Both results are in qualitative agreement with the findings of Photiadis,<sup>2</sup> although he concluded that Q is increased by a factor of  $R_0^{-1/2}$  relative to the rigid value whereas we find the larger factor of  $R_0^{-5/2}$ .

Using the above definitions,  $M_{\infty}$  may be expressed in resonance form,

$$M_{00} = \frac{2}{3} Z_{0K}^f \alpha \delta \left[ k_0^2 - k^2 - (i/Q) k_0^2 \right]. \tag{60}$$

The system of equations (39) can now be solved approximately by focusing on the n = m = 0 terms, to give

$$q_0 \approx (aR_0/M_{00})[p_0^{(rig)}].$$
 (61)

Also, at low frequency it follows from (29) that  $[p_0^{(rig)}] \approx -C_0$ , where  $C_0 = 1$  for an incident plane wave of unit amplitude. Combining these approximations with equation (43), the radiation associated with the Helmholtz resonance becomes quite simply

$$p^{(1)} \approx C_0 \left(\frac{k}{k_0}\right)^3 \left(\frac{Q^{-1}}{1 - (k/k_0)^2 - iQ^{-1}}\right) \frac{e^{ikr}}{kr}.$$
 (62)

The small-opening approximations (58) have been used in simplifying the numerator in (62).

It is instructive to recast this result within the context of lumped parameters systems, which are commonly used for Helmholtz resonators. First, we need to find the net volume flow near resonance. The radial velocity on the spherical surface r = a is best expressed using equation (11) rather than (17), since the latter does not capture the rapid variation near the mouth. Referring to (17) and (19), we have  $L^{-1}[p] \approx (1 - R_0^{-1})A_0$ , where  $A_0$  follows from (20), (41), and (42) as  $A_0 \approx \alpha R_0 q_0/2$ . The radial velocity then follows from equations (11), (44), and (46) as

$$w(\theta) \approx \begin{cases} \frac{q_0}{\sqrt{2}\sqrt{\cos\theta - \cos\alpha}}, & \text{on the mouth,} \\ -(\alpha/2)(1 - R_0)q_0, & \text{on the shell.} \end{cases}$$
(63)

The shell motion is therefore out of phase with the fluid motion in the mouth. The former is small in comparison with the latter, the ratio of the average velocities being  $\alpha^2(1-R_0)/4$ . However, the total fluxes are comparable, as can be seen by integrating the velocities in (63) over the respective surface areas and using the fact that  $\alpha$  is small, yielding

$$\frac{\text{inward flux of shell}}{\text{outward flux of mouth}} = 1 - R_0.$$
 (64)

Define the net volume flux out of  $r \le a$  per unit time as

$$\bar{w} = \int_{r=a} w \, dS$$
$$= 2\pi a^2 \alpha R_0 q_0. \tag{65}$$

We now rewrite Eq. (61) in the suggestive form

$$-p^{\rm inc} \approx \frac{M_{00}}{2\pi (a\alpha R_0)^2} \,\bar{w}.\tag{66}$$

Here we have used the low-frequency approximation  $[p_0^{(rig)}] = -p^{inc}$ . Equation (66) implies that the net volume flow is driven by the incident field. Using Eqs. (55), (57), and (60) this can be expressed in the form of a forced, single degree of freedom damped oscillator,

$$-p^{\rm inc} \approx (Z_{\rm HR} + r_{\rm A})\bar{w},\tag{67}$$

where

$$Z_{HR} = (-i\omega C_A)^{-1} - i\omega M_A, \tag{68a}$$

and

$$C_A = \frac{R_0 V}{\rho c^2}, \quad M_A = \frac{\rho \delta}{R_0^2 S}, \quad r_A = \frac{\rho c k^2}{4\pi}.$$
 (68b)

The parameter  $r_A$  is the radiation resistance for a monopole source.<sup>15</sup> It depends only upon the exterior acoustic medium and is independent of the nature of the monopole, in this case

an elastic Helmholtz resonator. The volume impedance of the resonator,  $Z_{HR}$ , contains a stiffness and a mass, but no dissipative term. One could add an internal dissipation to  $Z_{\rm HR}$ , but we neglect this here, preferring instead to focus on the elasticity effects. The effective compliance, or capacitance,  $C_A$ , and the effective inertia,  $M_A$ , are both similar to their standard forms for Helmholtz resonators, 15 but modified in the present circumstances by the elasticity parameter  $R_0$ . Note that the capacitance is decreased relative to the rigid value  $V/\rho c^2$ , but the mass is enhanced by a greater amount, with the net result that the resonant frequency  $\omega_0 = 1/\sqrt{C_A M_A}$  is lowered. The increased effective stiffness,  $1/C_A$ , and effective mass,  $M_A$ , appear at first glance to be counter to one's expectations. However, it should be kept in mind that the effective impedance  $Z_{HR}$  refers to the net volume flow  $\bar{w}$  of Eq. (65) and not the volume flow across the mouth, which equals  $\bar{w}/R_0 > \bar{w}$ . Similarly, the enhanced mass can be ascribed to the increase in kinetic energy associated with the greater volume of fluid entrained in the out of phase motions of the shell and the fluid in the mouth.

We conclude this section with an analysis of the scattering cross section near resonance. The far-field monopole radiation resulting from a compact volume source  $\bar{w}$  is

$$p^{(1)} = (-i\omega\rho/4\pi r)e^{ikr}\overline{w}.$$
 (69)

Eliminate  $\bar{w}$  between (67) and (69), and use  $p^{\rm inc} \approx C_0$ , to get

$$p^{(1)} \approx \frac{i\rho ck}{4\pi r} C_0 \frac{e^{ikr}}{Z_{HR} + r_4}. \tag{70}$$

It may be verified, using the identities of (67), that the scattered pressures of Eqs. (62) and (70) are identical near the resonant frequency  $\omega_0 = ck_0$ . It is interesting to note that right at resonance,

$$p^{(1)} \approx iC_0(e^{ikr}/kr),\tag{71}$$

which is *independent of the shell elasticity*. Hence the total scattering cross section at resonance,  $\sigma$ , which is dominated by the field  $p^{(1)}$ , is increased relative to the corresponding rigid resonator. Using Eq. (58a), we see that

$$\sigma/\sigma^{\text{rigid}} \approx R_0^{-1}$$
. (72)

This contrasts with Photiadis' finding of a reduction at resonance by a factor of  $R_0^4$ . The identity (71) for the strength of the scattered field at resonance can be found in Rayleigh's treatise of 1896. Subsequent papers by Lamb<sup>16</sup> and Rayleigh<sup>17</sup> discuss its generalization to arbitrary multipole resonators. Hence, the increase in scattering cross section is purely a consequence of the lowered resonance frequency and is completely independent of the intrinsic properties of the resonator.

# IV. NUMERICAL RESULTS AND DISCUSSION

Before considering an elastic resonator we first apply the asymptotic theory of the previous section to the rigid cavity. Ingard<sup>18</sup> reported some measured frequencies of a spherical cavity in air which may be compared with the predictions of Eq. (55). Ingard also provided comparisons with two other approximate theories in which the velocity field across the mouth was approximated as either uniform or

TABLE I. Resonance frequencies of a spherical resonator, a = 0.09 m,  $h = 10^{-3}$  m. From Ingard (Ref. 18). The acoustic speed has been taken as c = 340 m/s

Hole diameter (cm)	Measured resonance frequency (Hz)	Uniform distribution from Ref. 18	Deviation	Variable distribution from	This paper, Eqs. Deviation (56) and Deviation		
			%	Ref. 18	(%)	(73)	(%)
1.6	120	117	- 2.5	123	2.5	121	0.64
2.05	135	134	- 0.75	142	5.2	138.5	2.53
3.1	168	168	0	180	7.8	174	3.45
3.7	190	185.5	-2.27	202	6.3	192	0.92
3.82	195	189	<b>–</b> 3	206	5.65	195	0.11
4.9	224	216	<b>- 3.57</b>	242	7.4	225	0.36

with the distribution  $w = w_0(\cos \theta - \cos \alpha)^{1/2}$ . The theoretical expressions use the well-known formula for the resonance frequency of a rigid cavity

$$k_0 = \sqrt{S/V(h+\delta)},\tag{73}$$

where S is the area of the mouth, V the cavity volume, and  $\delta$  the "end correction" for the aperture neck. The thickness h is also included here and may be understood as the "neck" length. The numbers in Table I were calculated using Eq. (73) with the end correction of Eq. (56). Also shown are the experimental values reported by Ingard and the predictions of the two theories discussed by Ingard, which differ in their choice of an end correction  $\delta$ . It can be argued from Table I that the present theory is at least as good or better than the commonly used formula based upon the velocity being uniform across the aperture <sup>18,2</sup>

The curves in Figs. 2–9 summarize extensive numerical calculations for both rigid and elastic resonators. We have focused on the far-field backscattered amplitude for plane wave incidence as shown in Fig. 1. The far-field scattering amplitude is defined as

$$f(\theta) = \lim_{(r \to \infty)} (2r)^{(D-1)/2} e^{-ikr} (p - p^{\text{inc}}), \tag{74}$$

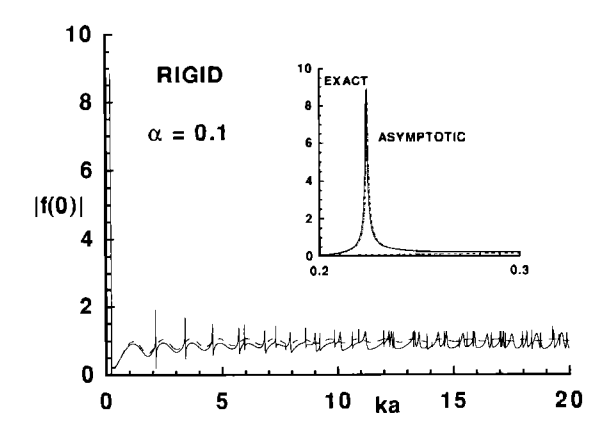


FIG. 2. The backscatter from a rigid cavity with  $\alpha=0.1$ . The dashed curve shows the response of a rigid sphere for comparison. Note the low-frequency Helmholtz resonance and the higher frequency cavity resonances. The average response at higher frequencies is decreased relative to the full sphere. The insert compares the Helmholtz resonance of the exact theory with the asymptotic approximation of Eq. (62) (dashed curve).

where D=3 or 2 is the appropriate dimensionality for the sphere or the cylinder (see Appendix C). Numerical results are presented here for D=3 only. The numerical computations required two truncations, at n=300 for the Legendre polynomial series, as in Eqs. (13) and (18), and a truncation for the series expansion (38) for the polarization. The latter was taken as n=12 and convergence checks were undertaken by comparing the results with smaller values, n=8 or n=10. In all cases the solution was found to converge to the degree of accuracy discernible in the graphs. These are referred to as the "exact" results, in contrast to some approximate calculations based upon the asymptotic results in the previous section.

The acoustic backscatter from rigid cavities of different apertures is illustrated in Figs. 2–5. Several aspects are worth noting. First, as expected, the Helmholtz resonance is the largest feature for small values of  $\alpha$ , see Figs. 2 and 3. Also, as Fig. 2 shows, the resonance is well approximated by the asymptotic theory of Sec. III for small apertures, although higher-order discrepancies can be seen in Fig. 3 for  $\alpha=0.25$ . In addition to the Helmholtz resonance there are obviously higher frequency "internal" resonances excited, which grow in significance as the aperture is increased. These modes are a combination of the pure modes inside the full, rigid container, modified by the access to the exterior region, of creeping waves, whispering gallery modes, and edge diffraction. Precise explanations for these are beyond the scope of this

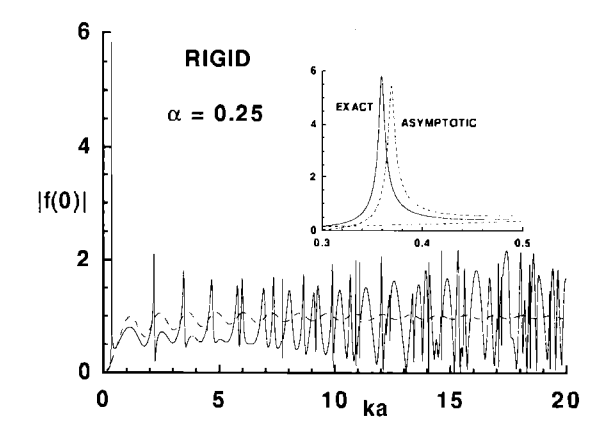


FIG. 3. The same as Fig. 2 but for the larger aperture  $\alpha = 0.25$ .

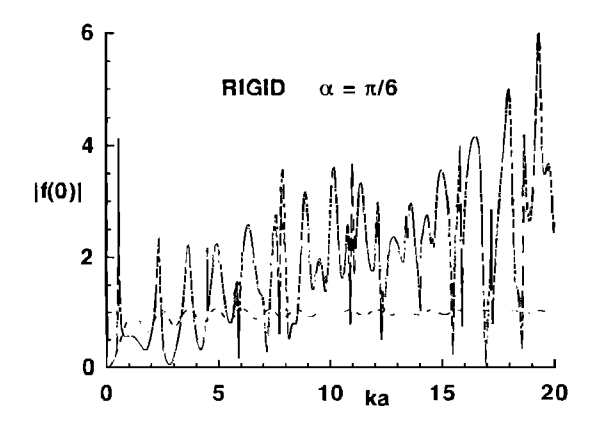


FIG. 4. The rigid backscatter for  $\alpha=\pi/6$ . Note the decrease in strength of the Helmholtz resonance and the stronger cavity modes. The general linear increase in the response with increasing frequency is suggestive of specular reflection—in this case from the inside of the sphere.

paper, but we note that for  $\alpha=\pi/6$ , for example, these higher frequency effects are comparable to or larger than the Helmholtz resonance. Furthermore, the overall response for larger mouths clearly shows the reflection of the plane wave from the inner concave surface. This is evident from the overall linear increase in amplitude as a function of ka, characteristic of specular reflection. Thus, for  $\alpha=\pi/3$ , although the Helmholtz resonance is the main feature for  $ka\leqslant 1$ , it is quickly dominated by high-frequency effects for ka>1. In contrast, the average high frequency response (ka>3) for  $\alpha=0.1$  in Fig. 2 appears to be consistently less than that for the full sphere. The hole in the sphere thus allows energy to enter the sphere, in the process causing a reduction in the specular return.

The remaining numerical results in Figs. 6-9 are for steel resonators in water, with c=1482.5 m/s,  $\rho=1000$  kg/m<sup>3</sup>,  $c_p=5431$  m/s,  $\rho_s=7700$  kg/m<sup>3</sup>,  $\nu=0.29$ , a/h=90, and the same range of values for  $\alpha$  considered in Figs. 2-5. No internal dissipation is included in the computations, the only loss mechanism is from radiation.

In comparing Figs. 2 and 6 it is clear that the Helmholtz resonance frequency has been decreased and the response at

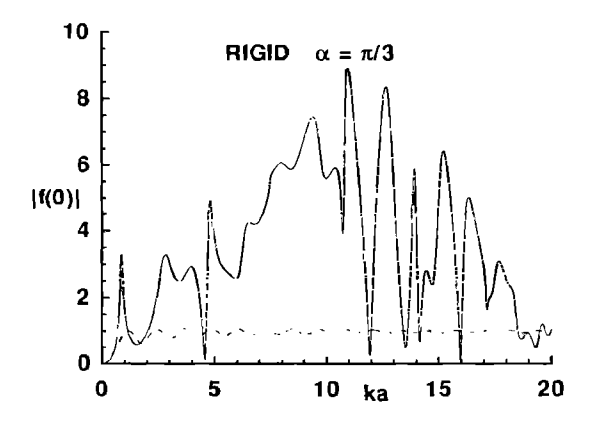


FIG. 5. The rigid sphere with  $\alpha=\pi/3$ . The Helmholtz resonance has virtually disappeared in comparison with the cavity modes, while the specular reflection effect is more pronounced.

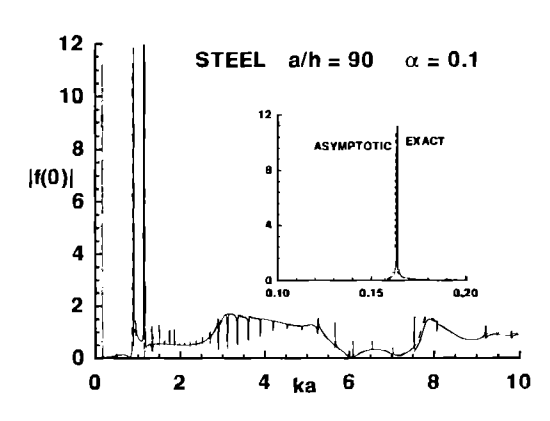


FIG. 6. The backscatter from a thin steel shell in water, a/h = 90,  $\alpha = 0.1$ . The two dominant shell modes near ka = 1 correspond to n = 2 and n = 3 in Table II, and their positions are accurately predicted using the conversion  $ka = 3.663 \Omega$ . The dashed curve showing the full shell response of Eq. (13) is difficult to distinguish, but may be more clearly seen in Figs. 7, 8, and 9. The insert compares the exact computations with the asymptotic theory of Eq. (62).

resonance is larger, with both effects accurately described by the asymptotic theory of the previous section. However, there are more striking differences at higher frequencies, ka = O(1), where the shell modes dominate the response of the elastic resonator. In particular, the full shell response displays strong resonances near ka = 1 and these resonances are more significant than the Helmholtz resonance itself, see Figs. 6 and 7. These relatively low-frequency structural modes are associated with the lower of the two branches predicted by ignoring the bending effects and keeping only the membrane effects in the thin shell theory. 19 The effect of fluid loading on these modes has been examined by Junger<sup>19</sup> and Strifors and Gaunaurd<sup>11</sup> for the case of one-sided loading from the exterior, but not for symmetric loading on both sides, which is the case of relevance to the Helmholtz resonator. We note that Strifors and Gaunaurd 10 have provided numerical results for the response of water-filled shells in water, but they do not discuss the quantitative nature of the low frequency resonances. In general, the fluid-loaded modal frequency of order n is given by the smaller root of the equation

$$\operatorname{Im}(Z_n^s + \hat{Z}_n) = 0, \tag{75}$$

where  $\hat{Z}_n$  is the fluid loading impedance. Three cases may be

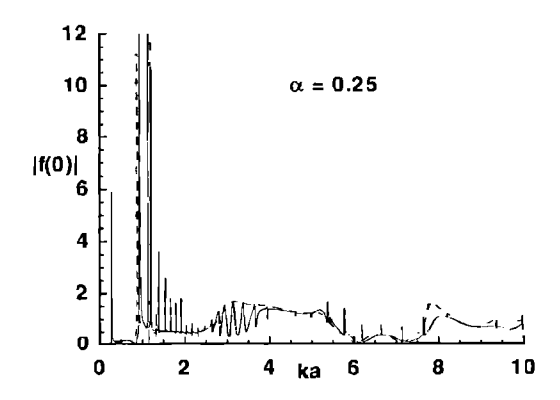


FIG. 7. The same steel shell of Fig. 6 but for the large aperture  $\alpha = 0.25$ .

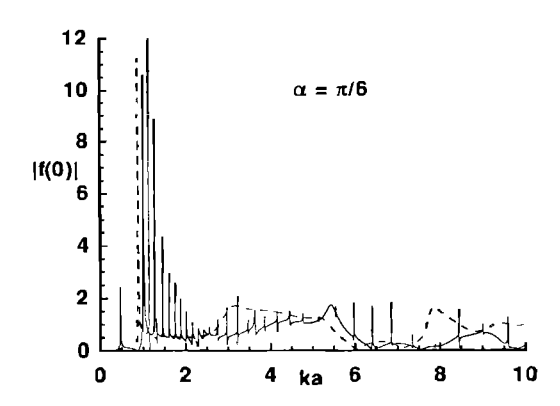


FIG. 8. The same as Fig. 7 but for  $\alpha = \pi/6$ .

distinguished: (i) no loading, for which  $\hat{Z}_n = 0$ ; (ii) one-sided loading on the exterior surface only,  $\hat{Z}_n = i\rho ch_n(ka)/h'_n(ka)$  [see Eq. (16)]; and two-sided loading by the same fluid,  $\hat{Z}_n = Z_n^f$  of (14). At the frequency range of interest the bending effects in the shell impedance may be ignored. Hence, using Eq. (A8) with  $\beta = 0$ , the frequency equation may be reduced to a transcendental equation in  $\Omega$  (Refs. 19 and 20),

$$\Omega^{4}(1+\eta\hat{m}_{n}) - \Omega^{2}[1+3\nu+\lambda_{n}+\eta\hat{m}_{n}(\lambda_{n}-1+\nu)] + (1-\nu^{2})(\lambda_{n}-2) = 0.$$
 (76)

The quantities  $\Omega$ ,  $\eta$ , and  $\lambda_n$  are defined in Appendix A, and we have introduced dimensionless radiation loss and inertance terms by  $\hat{Z}_n = \rho c(\hat{r}_n - ika\hat{m}_n)$ . Table II summarizes the results for the three cases. In general, the modal frequencies decrease as the fluid inertial loading is increased. The radiation loss  $\hat{r}_n$  is also included in Table II as it provides an estimate of the width of the associated resonance.

Is it possible for the Helmholtz resonance to coincide with the lowest of the structural resonances? In order to answer this it helps to focus on the dependence of both resonance frequencies on the same parameter, which we take as the fluid loading parameter  $\eta$  of Eq. (A3). The lowest structural frequency,  $\Omega = \Omega_2$ , where  $\Omega = kac/c_p$ , can be reasonably approximated from (76) by using the low-frequency estimate of  $\hat{m}_2 \sim 5/6$  from (47a). At the same time, we assume  $\eta$  is large, in fact  $\eta = 11.69$  in Table II. Then we find

$$\Omega_2^2 \approx \frac{4(1-\nu^2)}{7+3\nu+(5+\nu)5\eta/6}$$
(77)

This yields  $\Omega_2 \approx 0.2483$  as compared to  $\Omega_2 = 0.2423$  from Table II. At the same time, the Helmholtz resonance is at  $\Omega_{HR} = k_0 a c/c_\rho$ , which follows from (51) and (58a) as

$$\Omega_{\rm HR}^2 \approx \frac{\alpha}{\pi} \left( \frac{\eta}{1+\nu} + \frac{2}{3} \frac{c_p^2}{c^2} \right)^{-1}.$$
(78)

It is apparent from Eqs. (77) and (78) that both frequencies decrease as  $\eta$  increases. However, the Helmholtz resonance frequency is always much less than the lowest structural frequency because  $\alpha/\pi \ll 1$  by assumption. Hence, the two resonance phenomena will always be distinct and the answer to the above question is in the negative. These conclusions are consistent with the results of Figs. 6–9, which also show how the Helmholtz resonance disappears as  $\alpha$  becomes larger.

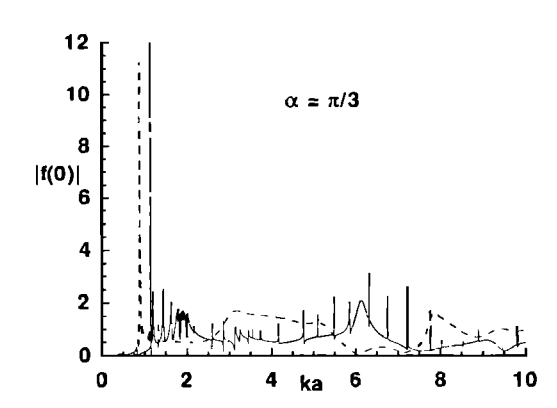


FIG. 9. The same as Fig. 7 but for  $\alpha = \pi/3$ .

Another obvious feature of Figs. 6–9 is the appearance of many sharp structural resonances. The first six or so of these for  $1 \le ka \le 2$  can be associated with the higher modes of Table II. The other modes for  $ka \ge 2$ , roughly, do not correspond to either solution branch of (76) but appear to be flexural waves on the shell. This conjecture is supported by the trend  $k_m a \sim m^2$  for these frequencies, which one would expect for higher-order standing waves of flexural type. We note that as the mouth size is increased the membrane modes become less significant in comparison with the bending modes. Also, the membrane modes are shifted to higher frequencies, which can be thought of in terms of the "effective" shell becoming smaller. We note that the flexural modes are all subsonic, in fact the coincidence frequency for this shell is at ka > 40. Also, the specular reflection effect, so apparent for the rigid cavity at larger values of  $\alpha$ , is missing in Figs. 8 and 9. This is simply explained by the small reflection coefficient for a thin steel plate in water at these frequencies.

#### V. CONCLUSIONS

A general theory for acoustic scattering from elastic Helmholtz resonators has been described and applied to the specific case of thin spherical shells with circular apertures. The resulting integral equation can be solved numerically and is amenable to asymptotic analysis for small mouth

TABLE II. The lower branch of the modal frequencies of a fluid-loaded spherical steel shell in water, a/h = 90.

Mode order	In vacuo	Loading on	exterior only	Loading on both side:		
n	$\Omega_n$	$\Omega_{u}$	r,	$\Omega_{"}$	î,	
1	0	0	0	0	0	
2	0.7049	0.3364	0.03742	0.2423	0.00561	
3	0.8338	0.4228	0.00740	0.3118	0.00071	
4	0.8842	0.4829	0.00084	0.3611	0.00005	
5	0.9089	0.5277	0.00006	0.4001	0	
6	0.9228	0.5631	0	0.4326	0	
7	0.9315	0.5923	0	0.4606	0	
8	0.9372	0.6169	0	0.4851	0	
9	0.9412	0.6382	0	0.5069	0	

sizes. The asymptotic results indicate that wall elasticity reduces the resonance frequency by a factor of  $R_0^{1/2}$  in comparison with a rigid cavity, where  $R_0 < 1$  is defined in Eq. (51). Both the Q value of the resonance and the scattering cross section are enhanced by the wall compliance, by factors of  $R_0^{-5/2}$  and  $R_0^{-1}$ , respectively. The increased scattering strength is a consequence of the lowered resonance frequency and is independent of the type of thin shell theory used. Numerical results for thin steel shells in water indicate that the asymptotic theory is adequate for describing the resonance behavior for small apertures, and for larger apertures the Helmholtz resonance is relatively insignificant in comparison with structural modes.

# **ACKNOWLEDGMENTS**

This work was supported by the U.S. Office of Naval Research. Computations were performed at the Pittsburgh Supercomputer Center, under a grant from the National Science Foundation, MSM91002P. The contribution of GRW was supported in part by the Applied Mathematical Sciences subprogram of the Office of Energy research, U.S. Department of Energy, under Contract No. W-7405-ENG-82.

# **APPENDIX A: SPHERICAL SHELL THEORIES**

Define the shell parameters

$$\beta^2 = h^2/12a^2, \quad \Omega = \omega a/c_n. \tag{A1}$$

Here, h and a are the shell thickness and radius, respectively, with  $h \le a$  by assumption. The plate speed  $c_p$  is

$$c_o^2 = E/\rho_s (1-v^2),$$
 (A2)

where E and  $\nu$  are the Young's modulus and Poisson's ratio, and  $\rho_s$  the density of the shell. The fluid loading on the shell may be characterized by the *fluid loading parameter* 

$$\eta = \rho a/\rho_{s}h. \tag{A3}$$

It is assumed for simplicity that there is no dependence upon the azimuthal angle  $\phi$ . Only one in-surface component is zero, the one associated with  $\theta$  and we denote it by u. Let  $\mu \equiv \cos \theta$ , then the operator L of (3) for the spherical shell is defined by

$$Lw = \frac{-i\rho_s h c_p^2}{\omega a^2}$$

$$\times \left(\Omega^2 w - 2(1+\nu)w - \beta^2 \nabla_\mu^2 (\nabla_\mu^2 + 1 - \nu)w + (1+\nu)\frac{d}{d\mu} (\sqrt{1-\mu^2}u)\right), \tag{A4}$$

where

$$\nabla_{\mu}^{2} = \frac{d}{d\mu} (1 - \mu^{2}) \frac{d}{d\mu} \,. \tag{A5}$$

The subsidiary equation for u is

$$(\Omega^{2} + 1 \quad \nu)u + \sqrt{1 - \mu^{2}} \frac{d^{2}}{d\mu^{2}} \times (\sqrt{1 - \mu^{2}}u) - (1 + \nu)\sqrt{1 - \mu^{2}} \frac{dw}{d\mu} = 0.$$
 (A6)

These are the shell equations of Green and Zerna<sup>21</sup> applied to a sphere. The equations are similar to those of Junger and Feit,<sup>20</sup> Eqs. (7.102), (7.103) et seq., which contain additional terms proportional to  $\beta^2$ . If we put  $w = P_n(\cos \theta)$ , then it is a simple matter to show that the impedance defined by Eq. (15) is

$$Z_n^s = \frac{i\rho c}{ka} \frac{c_\rho^2}{\eta c^2} \left( 2(1+\nu) - \Omega^2 + \beta^2 \lambda_n (\lambda_n - 1 + \nu) - \frac{\lambda_n (1+\nu)^2}{\lambda_n - 1 + \nu - \Omega^2} \right), \tag{A7}$$

where  $\lambda_n = n(n+1)$ . The effect of including the higher-order terms in the Junger and Feit equations<sup>20</sup> is that  $Z_n^s$  changes to

$$Z_{n}^{s} = \frac{i\rho c}{ka} \frac{c_{p}^{2}}{\eta c^{2}} \left( 2(1+\nu) - \Omega^{2} + \beta^{2} \lambda_{n} (\lambda_{n} - 1 + \nu) - \frac{\lambda_{n} \left[ 1 + \nu - \beta^{2} (1 - \nu - \lambda_{n}) \right]^{2}}{(\lambda_{n} - 1 + \nu) (1 + \beta^{2}) - \Omega^{2}} \right).$$
(A3)

Whether Green and Zerna's or Junger and Feit's equations are used, the tangential velocity field is of the form  $u = B_n \sin \theta P'_n(\cos \theta)$ . In the latter case,

$$B_n = \frac{1 + \nu - \beta^2 (1 - \nu - \lambda_n)}{\Omega^2 + (1 - \nu - \lambda_n)(1 + \beta^2)},$$
 (A9)

and for Green and Zerna's theory  $B_n$  is the same but with the  $\beta^2$  terms eliminated. The impedance function (A8) was used in the numerical computations discussed in Sec. IV, although it was found that (A7) gave identical curves for the cases considered.

# APPENDIX B: AN INFINITE SUM

The infinite sum in (53) may be determined as follows.

$$\sum_{n=1}^{\infty} \frac{\sin^{2}(n+\frac{1}{2})\alpha}{n(n+1)}$$

$$= \frac{1}{2} \sum_{n=1}^{\infty} \left( \frac{1}{n(n+1)} - \frac{1}{n(n+1)} \cos(2n+1)\alpha \right)$$

$$= \frac{1}{2} \left[ 1 - \sum_{n=1}^{\infty} \left( \frac{\cos(2n+1)\alpha}{n} - \frac{\cos(2n+1)\alpha}{n+1} \right) \right]$$

$$= \frac{1}{2} \left( 1 - \cos\alpha + \sum_{n=1}^{\infty} \frac{1}{n} [\cos(2n-1)\alpha - \cos(2n+1)\alpha] \right)$$

$$= \sin^{2} \frac{\alpha}{2} + \sin\alpha \sum_{n=1}^{\infty} \frac{\sin 2n\alpha}{n}.$$
(B1)

Then (53) follows using Eq. (1.448.1) of Ref. 22 for the infinite sum in (B1).

# APPENDIX C: THE CYLINDRICAL RESONATOR

The solution to (6) for the full shell subject to an incident wave of the form

$$p^{\text{inc}} = \sum_{n=0}^{\infty} C_n J_n(kr) \cos n\theta, \tag{C1}$$

is now

$$p^{(0)} = p^{\text{inc}} - \sum_{n=0}^{\infty} C_n \frac{Z_n^s}{Z_n^f + Z_n^s}$$

$$\times \cos n\theta \begin{cases} J_n(kr), & \text{for } r \leqslant a, \\ \frac{J_n'(ka)}{H_n'(ka)} H_n(kr), & \text{for } r \geqslant a. \end{cases}$$
(C2)

Here,  $H_n$  are Hankel functions of the first kind of order n and  $J_n$  are Bessel functions. The fluid impedances are

$$Z_n^f = \frac{2\rho c}{\pi ka J_n'(ka) H_n'(ka)},$$
 (C3)

and the solid impedances are the eigenvalues of

$$L\cos n\theta = Z_n^s \cos n\theta, \tag{C4}$$

for each  $n = 0, 1, 2, \dots$ . Again, the values of  $Z_n^s$  depend upon the shell theory used. Finally, we note that for the plane wave incidence traveling directly towards the mouth,  $p^{\text{inc}} = e^{-ikr\cos\theta}$ , the constants in (C1) are  $C_n = 2(-i)^n$ .

The mouth now has semi-angle  $\alpha$ , and is defined by  $-\alpha < \theta < \alpha$ , where  $-\pi < \theta \leqslant \pi$  is the polar angle about the center. The general solution may be split into the sum of parts which are symmetric and antisymmetric about the direction  $\theta = 0$ . We will only discuss the symmetric solution here, since it yields the Helmholtz resonance behavior. The antisymmetric solution could be handled in a similar manner but it would not exhibit the same resonance. The symmetric part of the radial velocity caused by the presence of the mouth can be expressed as

$$w^{(1)}(\theta) = \sum_{n=0}^{\infty} A_n \cos n\theta.$$
 (C5)

The fluid pressure then follows from (8) as

$$p^{(1)} = i\rho\omega \sum_{n=0}^{\infty} A_n \cos n\theta \begin{cases} \frac{H_n(kr)}{kH'_n(ka)}, & r > a, \\ \frac{J_n(kr)}{kJ'_n(ka)}, & r < a. \end{cases}$$
(C6)

The procedure is obviously very similar to that for a spherical shell. We will not repeat the steps analogous to (19)–(22), except to note that the coefficients  $A_n$  may be expressed in terms of the symmetric polarization  $W(\theta) = W(-\theta)$  as

$$A_n = \frac{\epsilon_n}{\pi} \frac{Z_n^s}{Z^f + Z^s} \int_0^\alpha W(\theta') \cos n\theta' \, d\theta', \qquad (C7)$$

where  $\epsilon_0 = 1$  and  $\epsilon_n = 2$ , n > 0. The resulting integral equation for  $W(\theta)$  over  $0 \le \theta \le \alpha$  becomes

$$\int_0^\alpha W(\theta')K(\theta,\theta')d\theta' = [p^{(0)}](\theta), \quad 0 \le \theta < \alpha. \quad (C8)$$

The kernel  $K(\theta, \theta') = K(\theta', \theta)$  is now

$$K(\theta, \theta') = \sum_{n=0}^{\infty} K_n \cos n\theta \cos n\theta', \tag{C9}$$

where

$$K_n = \frac{\epsilon_n}{\pi} \frac{Z_n^f Z_n^s}{Z_n^f + Z_n^s}.$$
 (C10)

The derivation of the matrix equations is slightly different than for the spherical case. We begin by assuming that the polarization may be represented as

$$W(\theta) = \frac{q(\theta)}{\sqrt{\alpha^2 - \theta^2}}.$$
 (C11)

This form contains the correct singularity near the edge, and means that the function  $q(\theta)$  should remain bounded for all  $\theta$ ,  $-\alpha \leqslant \theta \leqslant \alpha$ . Because we are only considering the symmetry problem, the range of interest is  $0 \leqslant \theta \leqslant \alpha$ . Comparing Eqs. (37) and (C11) it is clear that the function  $q(\theta)$  bears some similarity to the function for the spherical case.

With regard to (C8), we note that

$$\int_0^a W(\theta') \cos(n\theta') d\theta'$$

$$= \int_0^{\pi/2} q(\alpha \cos \phi) \cos(n\alpha \cos \phi) d\phi.$$
 (C12)

This suggests we try an expansion of  $q(\alpha \cos \phi)$  as a cosine series in  $\phi$ , or since  $\phi = \cos^{-1}(\theta/\alpha)$ , we assume

$$q(\theta) = \sum_{n=0}^{\infty} q_n \cos\left(2n\cos^{-1}\frac{\theta}{\alpha}\right). \tag{C13}$$

Note that  $\cos(2n\cos^{-1}x) = T_{2n}(x)$ , which are the Chebyshev polynomials. We have omitted the Chebyshev polynomials of odd order from the sum (C13) as these all have discontinuous slopes at  $\theta = 0$ . This makes them inadmissible because  $q(\theta)$ , being symmetric, should have zero slope at  $\theta = 0$ . Substituting the expansion (C13) into (C8) and (C12) reduces the integral equation to

$$\sum_{n=0}^{\infty} K_n \cos n\theta \sum_{m=0}^{\infty} p_{nm} q_m = [p^{(0)}](\theta), \quad 0 \leqslant \theta < \alpha,$$
(C14)

where now12

$$p_{ln} = \int_0^{\pi/2} \cos(2n\phi)\cos(l\alpha\cos\phi)d\phi$$
$$= (-1)^n (\pi/2)J_{2n}(l\alpha). \tag{C15}$$

We now expand the right member of (C14) as

$$[p^{(0)}](\theta) = \sum_{n=0}^{\infty} [p_n^{(0)}] \cos n\theta.$$
 (C16)

Next, multiply both sides of (C14) by  $T_{2m}(\theta/\alpha)/\sqrt{\alpha^2-\theta^2}$  and integrate over the mouth. This results in a system of linear equations for the unknowns  $q_m$  which is identical to the spherical case, i.e., Eqs. (39). The symmetric matrix M is again given by (40), where now  $p_{ln}$  are defined in Eq. (C15). We note that the coefficients  $[p_n^{(0)}]$  for the incident wave of Eq. (C1) are of the same form as those for the sphere, Eq. (28), where the rigid coefficients are now

$$[p_n^{\text{rig}}] = \frac{-i2C_n}{\pi k a H'_n(ka)}.$$
 (C17)

We note that the singular integral equation for the cylindrical resonator is similar to one obtained by Yang and Norris<sup>23</sup> in analyzing the scattering from a partially bonded fiber in a matrix. The same type of Helmholtz resonance occurs in that problem, but with different interpretations on the effective inertia and stiffness. Further discussion of the fiber resonance can be found in Refs. 24 and 25.

The cylindrical shell equations are<sup>20</sup>

$$Lw = \frac{-i\rho_s h c_p^2}{\omega a^2} \left( \Omega^2 w - w - \beta^2 \frac{d^4 w}{d\theta^4} - \frac{du}{d\theta} \right), \quad (C18)$$

where u is the tangential velocity in the direction of  $\theta$  and the other parameters are defined in Appendix A. The subsidiary equation for u is

$$\Omega^2 u + \frac{d^2 u}{d\theta^2} + \frac{dw}{d\theta} = 0.$$
 (C19)

The eigenvalue  $Z_n^s$  of Eq. (C4) can then be easily determined as

$$Z_{n}^{s} = \frac{-i\rho c}{ka} \frac{c_{p}^{2}}{nc^{2}} \left(\Omega^{2} - 1 + \frac{n^{2}}{n^{2} - \Omega^{2}} - \beta^{2} n^{4}\right).$$
 (C20)

The asymptotic analysis of the resonance follows the same lines as that of the sphere. The major details are summarized here. The impedances follow from Eqs. (C3) and (C20) as

$$Z_0^f = i \frac{\rho c}{ka} \times 2 \left( 1 - (ka)^2 \Lambda(ka) - i \frac{\pi}{4} (ka)^2 + o((ka)^2) \right),$$
(C21a)

$$Z_n^f = -i\rho cka \frac{2}{n} + O((ka)^3), \quad n>1,$$
 (C21b)

where

$$\Lambda(ka) = \frac{1}{6} [1 - 4\gamma - 4 \log(ka/2)], \tag{C22}$$

y is Euler's constant, and

$$Z_{0}^{s} = i \frac{\rho c}{ka} \left( \frac{c_{p}^{2}}{\eta c^{2}} - \frac{1}{\eta} (ka)^{2} + \cdots \right),$$

$$Z_{n}^{s} = i \frac{\rho c}{ka} \left[ \frac{c_{p}^{2}}{\eta c^{2}} \beta^{2} n^{4} - \frac{1}{\eta} \left( 1 + \frac{1}{n^{2}} \right) (ka)^{2} + O((ka)^{4}) \right], \quad n \ge 1.$$
(C23b)

Applying these approximations we find

$$M_{00} \approx (\pi/2)D(\alpha)Z_{0K}^{f}[F(ka,\alpha) - (ka)^{2}(1+iQ^{-1})],$$
 (C24)

where

$$F(ka,\alpha) = \frac{R_0}{2D(\alpha)}$$

$$\times \left[1 - (ka)^2 \left( (1 - R_0) \frac{c^2}{c_p^2} + R_0 \Lambda(ka) \right) \right],$$
(C25a)

$$Q = \frac{8D(\alpha)}{\pi R_0^2},\tag{C25b}$$

$$D(\alpha) = \sum_{n=1}^{\infty} \frac{J_0^2(n\alpha)}{n}.$$
 (C25c)

Quantities like  $Z_{0K}^f$  have the same meaning as before, although different values, and  $R_0$  is again defined by Eq. (51). The main difference compared with the spherical resonator is the presence of the logarithmic term. Also, the sum  $D(\alpha)$  cannot be reduced to a simple expression, but it can be asymptotically approximated for small  $\alpha$ ,<sup>24</sup>

$$D(\alpha) = \log(2/\alpha) + O(\alpha^2), \quad \alpha \le 1.$$
 (C26)

The resonance frequency is given by the root of  $F(ka,\alpha) - (ka)^2 = 0$ , which simplifies for small apertures to

$$2 \log \frac{2}{\alpha} = \frac{1}{(ka)^2} + \frac{R_0}{2} \times \left(\gamma - \frac{1}{4} + \log \frac{ka}{2}\right) + (1 - R_0) \frac{c^2}{c_\rho^2}.$$
 (C27)

Norris and Yang<sup>24</sup> obtained a formula for the resonance frequency of a fiber partially attached to an elastic matrix, and their Eq. (34) agrees with (C27) in the rigid limit  $(R_0 = 1)$ . Taking the leading order approximation to the root of (C27), the resonance frequency and the Q value may be expressed as

$$k_0 = \sqrt{\frac{R_0 S}{V \delta}}, \quad Q = \frac{8}{R_0 k_0^2 V},$$
 (C28)

where  $S=2a\alpha$  and  $V=\pi a^2$  are the two-dimensional analogs of the aperture area and cavity volume, and the "end correction" is

$$\delta = (2/\pi)a\alpha D(\alpha)$$

$$\approx (2/\pi)a\alpha \log (2/\alpha). \tag{C29}$$

Finally, we note that the scattered field near resonance can be approximated as

$$p^{(1)} \approx \frac{iQ^{-1}C_0H_0(kr)}{F(ka,\alpha) - (ka)^2(1+iQ^{-1})}.$$
 (C30)

Hence, right at the resonance the response is

$$p^{(1)} \approx -C_0 H_0(kr),$$
 (C31)

which is similar in its simplicity to the three-dimensional result (71).

<sup>&</sup>lt;sup>1</sup> J. W. S. Rayleigh, *The Theory of Sound* (Dover, New York, 1945), Vol. 2.
<sup>2</sup> D. M. Photiadis "The effect of wall elasticity on the properties of a Helman

<sup>&</sup>lt;sup>2</sup> D. M. Photiadis, "The effect of wall elasticity on the properties of a Helmholtz resonator," J. Acoust. Soc. Am. 90, 1188-1190 (1991).

<sup>&</sup>lt;sup>3</sup>J. W. S. Rayleigh, "The theory of the Helmholtz resonator," Proc. R. Soc. London Ser. A **92**, 265–275 (1916).

<sup>&</sup>lt;sup>4</sup>H. Levine, "The wavelength of a spherical resonator with a circular aperture," J. Acoust. Soc. Am. 23, 307-311 (1951).

<sup>&</sup>lt;sup>5</sup>T. A. Henriquez and A. M. Young, "The Helmholtz resonator as a high-power deep-submergence source for frequencies below 500 Hz," J. Acoust. Soc. Am. 67, 1555–1558 (1980).

<sup>6</sup> M. S. Howe, "On the Helmholtz resonator," J. Sound Vib. 45, 427-440 (1976).

<sup>&</sup>lt;sup>7</sup>U. Ingard, "On the theory and design of acoustic resonators," J. Acoust. Soc. Am. 25, 1037–1061 (1953).

<sup>&</sup>lt;sup>8</sup>G. Wickham, "A general theory of scattering by thin interface layers, plates and shells," submitted for publication to Wave Motion (1992).

- <sup>9</sup>G. C. Gaunaurd and M. F. Werby, "Acoustic resonance scattering by submerged elastic shells," Appl. Mech. Rev. **43**, 171–207 (1990).
- <sup>10</sup> H. C. Strifors and G. C. Gaunaurd, "Differences in the acoustic echoes from submerged elastic shells containing different fluids," Ultrasonics 30, 107-112 (1992).
- <sup>11</sup> H. C. Strifors and G. C. Gaunaurd, "Multipole character of the large-amplitude, low frequency resonances in the sonar echoes of submerged spherical shells," Int. J. Solids Struct. 29, 121–130 (1992).
- <sup>12</sup> M. Abramowitz and I. Stegun, *Handbook of Mechanical Functions* (Dover, New York, 1972).
- <sup>13</sup> P. M. Morse and H. Feshbach, *Methods of Theoretical Physics* (McGraw-Hill, New York, 1953).
- <sup>14</sup> S. S. Vinogradov, Y. A. Tuchkin, and V. P. Shestopalov, "On the theory of scattering of waves by nonclosed screens of spherical shape," Sov. Phys. Dok. 26, 169–171 (1981).
- <sup>15</sup> A. D. Pierce, Acoustics: An Introduction to its Physical Principles and Applications (Acoustical Society of America, Woodbury, NY, 1989).
- <sup>16</sup> H. Lamb, "A problem in resonance, illustrative of the theory of selective absorption of light," Proc. London Math. Soc. 32, 11–20 (1900).

- <sup>17</sup> J. W. S. Rayleigh, "Some general theorems concerning vibrations and resonance," Philos. Mag. 3, 97–117 (1902).
- <sup>18</sup> U. Ingard, "The near field of a Helmholtz resonator exposed to a plane wave," J. Acoust. Soc. Am. 25, 1062–1067 (1953).
- <sup>19</sup> M. C. Junger, "Normal modes of submerged plates and shells," in *Fluid-Solid Interaction*, edited by J. E. Greenspon (ASME, New York, 1967), pp. 79-119.
- <sup>20</sup> M. C. Junger and D. Feit, Sound Structures and Their Interaction (MIT, Cambridge, MA, 1972).
- <sup>21</sup> A. E. Green and W. Zerna, *Theoretical Elasticity* (Oxford U.P., London, UK, 1968).
- <sup>22</sup> I. S. Gradshteyn and I. M. Ryzhik, Tables of Integrals, Series and Products (Academic, New York, 1980).
- <sup>23</sup> Y. Yang and A. N. Norris, "Shear wave scattering from a debonded fibre," J. Mech. Phys. Solids 39, 273-294 (1991).
- <sup>24</sup> A. N. Norris and Y. Yang, "Dynamic stress on a partially bonded fiber," J. Appl. Mech. 58, 404–409 (1991).
- <sup>25</sup> Y. Yang and A. N. Norris, "Longitudinal wave scattering from a partially bonded fiber," Wave Motion 15, 43-59 (1992).